Understanding the Structure of Aqueous Cesium Chloride Solutions by Combining Diffraction Experiments, Molecular Dynamics Simulations, and Reverse Monte Carlo Modeling

Viktória Mile,[†] László Pusztai,*[,†] Hector Dominguez,[‡] and Orest Pizio[§]

Research Institute for Solid State Physics and Optics, Hungarian Academy of Sciences, H-1525 Budapest, P.O. Box 49, Hungary, Instituto de Investigaciones en Materiales, Universidad Nacional Autonoma de Mexico (UNAM), Circuito Exterior s/n., Coyoacán, México, D. F. 04510, and Instituto de Quimica, UNAM, Circuito Exterior, Coyoacán, México, D. F. 04510

Received: January 5, 2009; Revised Manuscript Received: June 5, 2009

A detailed study of the microscopic structure of an electrolyte solution, cesium chloride (CsCl) in water, is presented. For revealing the influence of salt concentration on the structure, CsCl solutions at concentrations of 1.5, 7.5, and 15 mol % are investigated. For each concentration, we combine total scattering structure factors from neutron and X-ray diffraction and 10 partial radial distribution functions from molecular dynamics simulations in one single structural model, generated by reverse Monte Carlo modeling. This combination of computer modeling methods is capable of (a) showing the extent to which simulation results are consistent with experimental diffraction data and (b) tracking down distribution functions in computer simulation that are the least comfortable with diffraction data. For the present solutions, we show that the level of consistency between simulations that use simple pair potentials and experimental structure factors is nearly quantitative. Remaining inconsistencies seem to be caused by water−water distribution functions. Changing the pair potentials of water−water interactions from SPC/E to TIP4P-2005 has not had any effect in this respect. As a final result, we obtained particle configurations from reverse Monte Carlo modeling that were in quantitative agreement with both diffraction data and most of the molecular dynamics (MD) simulated partial radial distribution functions (prdf's). From the particle coordinates, the distribution of the number of first neighbors, as well as angular correlation functions, were calculated. The average number of water molecules around cations decreases from about 8 to about 6.5 as concentration increases from 1.5 to 15 mol %, whereas the same quantity for the anions changes from about 7 to about 5. It was also found that the average angle of Cl···H−O particle arrangements, characteristic of anion−water hydrogen bonds, is closer to 180° than that found for O···H−O arrangements (water−water hydrogen bonds). The present combination of experimental and computer simulation methods appears to be promising for the study of other electrolyte solutions.

1. Introduction

Electrolyte solutions are present and important in many areas of our lives. On one hand, they serve as media for various biological processes; on the other hand, their technical/industrial role is also outstanding. Aqueous electrolytes have been frequently chosen as subjects of experimental and theoretical studies.

Despite huge efforts for understanding various properties of electrolyte solutions over the past four decades,[1] they are still challenging from the point of view of their microscopic structure. The main difficulty concerning diffraction measurements is that even the simplest such solution contains four different scattering centers (anion, cation, oxygen, hydrogen). That is, for determining the full set (i.e., 10) of partial radial distribution functions (prdf's) one would need 10 independent experimental total scattering structure factors (tssf's)—which is clearly a task that can never be completed in practice. Computer simulation methods,[2] on the other hand, can provide detailed descriptions of the structure; unfortunately, here one has to deal with the problem of choosing appropriate interaction potentials.[1,2] It can be concluded that neither diffraction experiments nor computer simulations are omnipotent with respect to the description of the structure of electrolyte solutions.

Very recently, a scheme was proposed[3] for combining results of diffraction experiments [in the form of the primary information, the total scattering structure factor (tssf)] and molecular dynamics (or Monte Carlo) computer simulations (using partial rdf's resulting from them). The approach was originally designed for allowing a quantitative assessment of the capabilities of a given interaction potential from the point of view of the structure. In this spirit, it was possible to establish in the pilot study mentioned[3] that out of two aqueous solutions of rubidium bromide the molecular dynamics (MD) simulated structure of the 2*m* (about 4 mol %) one showed much better consistency with neutron diffraction data than that of the concentrated (5*m*, corresponding to about 10 mol %) solution (for details, see refs 3 and 4). In a follow-up investigation of eight interaction potential models of water,[5] the consistency between these potentials and the neutron diffraction data on heavy water[6] was considered. It was found that while none of the pair interaction models was perfect, most of them performed better than expected.

Here, we wish to apply the scheme[3] for revealing the microscopic structure of a rather suitable prototype of electrolyte

* Corresponding author. E-mail: lp@szfki.hu. Tel./Fax: +36 1 392 2589.
† Hungarian Academy of Sciences.
‡ Instituto de Investigaciones en Materiales, UNAM.
§ Instituto de Quimica, UNAM.

10.1021/jp900092g CCC: $40.75 © 2009 American Chemical Society
Published on Web 07/09/2009

TABLE 1: Contributions of Partial Structure Factors to the Neutron- and X-ray Weighted Total Scattering Structure Factors (Normalized, so That the Sum of the Contributions Equals Unity)[a]

c/mol %	Cs−Cs	Cs−Cl	Cs−O	Cs−H	Cl−Cl	Cl−O	Cl−H	O−O	O−H	H−H
0.0 (X)								0.65; 0.92	0.31; 0.08	0.04; 0.00
0.0 (N)								0.091	0.42	0.49
1.5 (X)	0.0; 0.02	0.0; 0.01	*0.11*; *0.26*	*0.03*; *0.01*	0.0; 0.0	0.03; *0.05*	0.0; 0.0	*0.52*; *0.61*	*0.26*; 0.02	0.03; 0.0
1.5 (N)	1.80×10^{-5}	6.35×10^{-5}	0.00254	0.00584	5.61×10^{-5}	0.00449	0.01032	*0.08973*	*0.41261*	*0.47433*
7.5 (X)	0.08; *0.21*	0.05; 0.1	*0.28*; *0.38*	0.07; 0.01	0.01; 0.01	*0.09*; 0.09	0.02; 0.0	*0.25*; *0.18*	0.03; 0.01	0.01; 0.0
7.5 (N)	0.00047	0.00165	0.01233	0.02835	0.00146	0.02179	0.05009	*0.08120*	*0.37340*	*0.42926*
15 (X)	*0.18*; *0.36*	*0.11*; *0.17*	*0.30*; *0.29*	0.07; 0.0	0.02; 0.02	0.09; 0.08	0.02; 0.0	*0.12*; 0.06	0.06; 0.0	0.0; 0.0
15 (N)	0.00195	0.00688	0.02348	0.05397	0.00607	0.04148	*0.09537*	0.07082	*0.32564*	*0.37435*

[a] For X-ray diffraction, these weighting factors depend on the value of the scattering variable, Q, and therefore, contributions at two Q values, at 0 and 10 Å^{-1} are provided (separated by semicolons). Note that for neutron diffraction (but *not* for X-ray diffraction), the same weighting factors are valid for the partial radial distribution functions in r-space. For the sake of comparison, weighting factors for pure water are also given. N: neutron diffraction. X: X-ray diffraction. The top three contributions are highlighted in italics for each case.

solutions (see below for details), the solution of cesium chloride in water. We will complement diffraction data with simulation results, in order to provide detailed structural models, as a function of salt concentration, that are consistent (within experimental errors) with neutron and X-ray diffraction data and as close as possible to results of computer "experiments". The advantage of such structures is that they are constructed by using all the available underlying physical observations. Simultaneously, detailed information concerning the applicability of the particular set of pair potential parameters for describing the structure of CsCl solutions will be obtained. The major difference of our approach from another structural modeling scheme, the "Empirical Potential Structure Refinement" method,[7] which has been frequently applied to electrolyte solutions (see, e.g., ref 8), is that we do not adjust values for the potential parameters. Instead, we explore different available models for the solvent.

While studying electrolyte solutions another principal difficulty—besides the number of distribution functions—is that the contributions of the dissolved ions to the total scattering pattern are frequently low, due to the low ionic concentration, as well as to the low scattering power of the ions. Neutron diffraction signals are always dominated by water contributions (see Table 1), and in many cases, this statement is valid for X-ray diffraction too, since the ions that are most important in practice (Li^+, Na^+, K^+, Ca^{2+}, or Cl^-) have relatively few electrons. Therefore, they are not much better X-ray scatterers than water. For the most effective exploitation of the potentialities of diffraction methods, solutions that are optimal in terms of concentration and scattering power, as well as in terms of contrast between neutron and X-ray diffraction, must be chosen. This is how and why the subjects of the present investigation, aqueous cesium chloride solutions, have been selected.

Cesium ions have 54 electrons, and therefore, the cation−oxygen contribution to the X-ray diffraction pattern is considerable even at low concentration (see Table 1). Cation−cation and cation−anion contributions are exceptionally high for X-ray diffraction at higher concentration values, whereas neutron diffraction data still contain (for deuterated samples) mostly O−D and D−D contributions. Also, CsCl dissolves very well in water at room temperature: a concentration of 15 mol % can easily be achieved. The hydration structure around the ions in such a case, where the solubility range is extremely wide, must be concentration dependent: at low concentration, the probability that an ion has a "full" (or "perfect", undisturbed) hydration shell is much higher than at higher concentrations (close to saturation). At very high concentrations, the hydration shells are likely to be distorted, not at least due to the relative shortage of water molecules. Highly concentrated aqueous CsCl solutions may thus also serve as a prototype of "concentrated" solutions, where the hydration structure, as well as the structure of the solvent subsystem, may be strongly deformed. It is interesting to note here that despite their favorable features from the experimental point of view the structure of CsCl solutions—to our best knowledge—has not been previously investigated experimentally. Concerning the hydration of Cs^+ and Cl^- ions in other systems, references will be given while comparing results of the present study with previous findings, in section 3.

In the present work, aqueous solutions of cesium chloride over a wide range of concentration, at 1.5, 7.5, and 15 mol % (one Cs^+ and one Cl^- ion per 66, 12, and 6 water molecules, respectively), are considered. In the next section, computational details concerning molecular dynamics simulation and reverse Monte Carlo (RMC) modeling[9] are described. In section 3, results and their discussion are provided, while section 4 summarizes our findings.

2. Computational Methods

2.1. Molecular Dynamics Simulation. We have carried out molecular dynamics simulations in the canonical (N,V,T) ensemble (with a Hoover thermostat) using the DL_poly software.[10] A rigid water model, SPC/E,[11] was applied first, while the ionic interactions were mimicked by a "Coulomb-plus-Lennard-Jones" parameter set,[12−14] so that the pair potential energy function between the ith and the jth particles took the following general form:

$$V_{ij}(r) = \frac{q_i q_j}{r_{ij}} + \frac{A_i A_j}{r_{ij}^{12}} - \frac{B_i B_j}{r_{ij}^{6}} \qquad (1)$$

In eq 1, q_i are charges on the interaction sites whereas A_i and B_j are the Lennard-Jones parameters. The A_i and B_j pair potential parameters for the ion−water pairs were taken from ref 12. Knowing SPC/E parameters, ion−ion parameters were extracted by employing Lorentz−Berthelot mixing rules. The particle mesh Ewald method (with a precision of 10^{-4}) was employed for calculating long-range Coulomb forces, whereas van der Waals interactions were cut off at 10 Å; periodic boundary conditions were imposed in all directions. In order to survey possible effects of the water potential model, the same set of calculations was repeated by using the rigid water model TIP4P-2005.[15] In this case, parameters for ion−water interactions were calculated based on the ion−ion parameters derived previously and applying Lorentz−Berthelot mixing rules again. It would be desirable to explore flexible water models along the present

TABLE 2: Some Parameters of the MD and RMC Calculations

salt concentration (mol %)	1.50	7.49	15.061
number density	0.0978	0.0877	0.08071
density (g/cm^3)	1.21	1.55	1.99
number of particles (MD)	2800	3153	3333
number of particles (RMC)	10000	10000	10001
box length (RMC; in Å)	46.78	48.46	49.84
maximum move (RMC)	0.1	0.1	0.1
units of (1 cation + 1 anion)/ H_2O molecules	50/3300 = 0.0152	257/3162 = 0.0813	529/2981 = 0.177

line of research; for the much higher computational demand, such a study will be the subject of future work.

The number of particles and the density for each calculation can be found in Table 2. Equilibration last for at least 1.5 ns and production runs started after another 1 ns, using a time step of 2 fs. Partial radial distribution functions have been calculated by averaging over 1000 configurations, sampled after reaching equilibrium, at each concentration.

2.2. Reverse Monte Carlo Modeling. As details of the reverse Monte Carlo method have been described in several publications,[9,16−18] here we only provide practical details, focusing on the features that are essential concerning the purpose of this work.

Reverse Monte Carlo is a simple tool for constructing large, three-dimensional structural models that are consistent with the total scattering structure factors (within the estimated level of their errors) obtained from diffraction experiments. Via random movements of particles, the difference between experimental and model total structure factors (calculated similarly to the χ^2-statistics) is minimized. As a result, by the end of the calculation particle configurations are available that are consistent with the experimental structure factor(s). If the structure is to be analyzed further, partial radial distribution functions, as well as other structural characteristics (neighbor distributions, cosine distribution of bond angles) can be calculated from the particle configurations.

For the present purpose, the most attractive feature of the RMC method is that it can take any external information that can be calculated directly from the coordinates of the particles. Partial radial distribution functions from MD simulations are this type of information. If consistency with all input data is reached, then it may be stated that the different pieces of input data are consistent with each other, as well as with the resulting particle configurations.

If, on the other hand, some of the input data cannot be approached within their uncertainties then it means that parts of the input data set are not consistent with other pieces of input information. In our case, this would mean that some of the input prdf's from MD would not be consistent with the experimental input total scattering structure factors. The resulting RMC particle configurations would still be consistent with experimental data and with some of the input prdf's. For the partial radial distribution functions, the modeling background, the pair potential, is known. Thus, these configurations would still represent enhanced structural models of aqueous CsCl solutions, over a wide range of concentration.

In the RMC calculations that are important ingredients of the present research, the experimental data set consists of two total scattering structure factors: one from neutron and one from X-ray diffraction.

It may be helpful to note here that total scattering structure factors for the case of neutron diffraction are defined throughout this work via the following equations:[19]

$$G^{\mathrm{N}}(r) = \sum_{i,j=1}^{n} b_i b_j c_i c_j [g_{ij}(r) - 1] \tag{2a}$$

$$F^{\mathrm{N}}(Q) = \rho_0 \int_0^{\infty} 4\pi r^2 G^{\mathrm{N}}(r) \frac{\sin Qr}{Qr}\, \mathrm{d}r \tag{2b}$$

In eqs 2a and 2b, c_i and b_i are the molar ratio and the scattering length of species i, $g_{ij}(r)$ are the partial radial distribution functions, $G^{\mathrm{N}}(r)$ is the total radial distribution function, ρ_0 is the number density of the system, and Q is the scattering variable (proportional to the scattering angle); indexes i and j run through species of the system. For X-ray diffraction, the quantity that has the role of b_i, the so-called atomic form factor, $f_i(Q)$, depends on the value of the scattering variable Q, and therefore, the composition of the X-ray weighted tssf in reciprocal space has the form of

$$F^{\mathrm{X}}(Q) = \sum_{i,j=1}^{n} f_i(Q) f_j(Q) c_i c_j [A_{ij}(Q) - 1] \tag{3}$$

where $A_{ij}(Q)$ are the partial structure factors that are Fourier-transforms of the partial radial distribution functions $g_{ij}(r)$. Because of the Q-dependence of the weighting factors for X-ray diffraction, the Fourier transform of $F^{\mathrm{X}}(Q)$, the X-ray weighted total radial distribution function, $G^{\mathrm{X}}(r)$, can only be interpreted in a qualitative manner. For a precise evaluation of $F^{\mathrm{X}}(Q)$ in real space, one needs to decompose it to partials in reciprocal space and take the Fourier-transform of the partials to obtain the partial radial distribution functions, $g_{ij}(r)$. This procedure can only be realized via inverse methods, like RMC.

Experimental data (neutron and X-ray weighted total structure factors) were taken from a recent comprehensive diffraction study on aqueous Rb- and Cs-halides; details of the experiments and the complete set of data will be published separately.[20] The same, deuterated, samples were applied for both neutron and X-ray diffraction experiments; this way, both the strong incoherent inelastic background of ^{1}H as well as any mismatch in terms of sample composition could be avoided. Neutron diffraction measurements have been conducted by using the SLAD liquids and amorphous diffractometer (NFL Studsvik, Sweden).[21] X-ray diffraction experiments have been performed at the SPring-8 synchrotron facility (Japan), using the high energy X-ray diffraction beamline BL04B2.[22] Data analyses for obtaining total scattering structure factors were carried via standard procedures.[21,23]

The other, "quasi-experimental", set of input information for RMC modeling, the set of simulated partial radial distribution functions, was provided by molecular dynamics simulations, as described in section 2.1. During the reverse Monte Carlo calculations that provided the structural models for further geometrical analyses, we required perfect agreement (within experimental uncertainties) with diffraction data and wanted to see how many of the potential-based partial rdf's could be fitted at the same time. This way, one (family) of the many particle arrangements that are consistent with a given set of diffraction data was selected—one whose physical background is represented by the interaction potentials applied in the MD simulation.

TABLE 3: Input Data for the Different (GR, FQ, GR_OK, FQ_OK) RMC Calculation Schemes[a]

	GR	FQ	GR_OK	FQ_OK
input ND total scattering structure factor	−	+	+	+
input XRD total scattering structure factor	−	+	+	+
input MD $g_{ij}(r)$'s	+	−	+	+
tight fit to measured data (within errors)	−	+	−	+
tight fit to $g_{ij}(r)$'s (within errors)	+	−	+	−

[a] ND: neutron diffraction. XRD: X-ray diffraction. Note that both the GR_OK and the FQ_OK schemes contain explicit fitting of both the experimental and MD input information; the difference between these two lies only in the different weights of these input data (see text for details).

The number of prdf's from the MD simulation has been increased gradually, for being able to monitor step-by-step whether any serious inconsistency occurs as a new prdf is introduced. The final pool of prdf's contained all the 10 $g_{ij}(r)$'s for the higher concentrated samples (7.5 and 15 mol %), whereas at the lowest concentration (1.5 mol %), the three ion−ion prdf's (Cs−Cs, Cs−Cl, and Cl−Cl) had to be left out because of the poor statistics. Note that the ion−ion prdf's have a combined weight below 1% in the diffraction signals, and thus, their omission does not represent any noticeable loss of information.

Technical details (density, system size) of the RMC calculations are provided in Table 2. In each calculation, more than one million moves were accepted while the average acceptance ratio varied between 30 and 40%. For exploratory purposes, we have carried out RMC modeling with no experimental input but using only prdf's from MD (denoted as "GR" from this point on) on one hand and with no prdf's but only experimental data as input (denoted as "FQ" from this point on) on the other hand. Also, many different runs were completed where both experimental and MD inputs were considered, with varying requirements concerning which data should be fitted closest. Apart from the already introduced GR and FQ data, throughout the rest of this report, we will only mention two of the hybrid calculations: the first one is when a perfect fit to MD prdf's was intended (denoted as "GR_OK" from this point on) and the second one is when a perfect fit to experimental data was required (denoted "FQ_OK: from this point on). In Table 3, the input data for the different (GR, FQ, GR_OK, FQ_OK) schemes are summarized.

We would finally like to mention that different interaction potential parameters may lead to different input partial rdf's; this assumption was tested by applying two different water potentials (see section 2.1). Note, however, that for the ionic parameters the choice is rather limited (see ref 12).

3. Results and Discussion

Figure 1 compares RMC simulated and experimental neutron and X-ray weighted total scattering structure factors at each concentration, using the FQ and FQ_OK calculations. It is obvious that no doubts can be raised concerning "goodness-of-fit" to experimental data; i.e., the particle configurations resulting from these two types of calculations are consistent with diffraction experiments within errors.

All the 10 partial radial distribution functions calculated from the particle coordinates of the FQ model and from the MD simulation using the SPC/E water potential are shown in Figure 2 for the highest salt concentration—15 mol %—case. The situation for the diluter solutions is similar. (Note that prdf's from the GR model are practically the same as those from the MD simulation.) It is clear that one cannot accept prdf's from the FQ model as physically meaningful: the curves, while showing hardly any recognizable feature, look rather messy with unphysical oscillations and other sudden intensity changes. This, perhaps unexpected, behavior can easily be understood if one

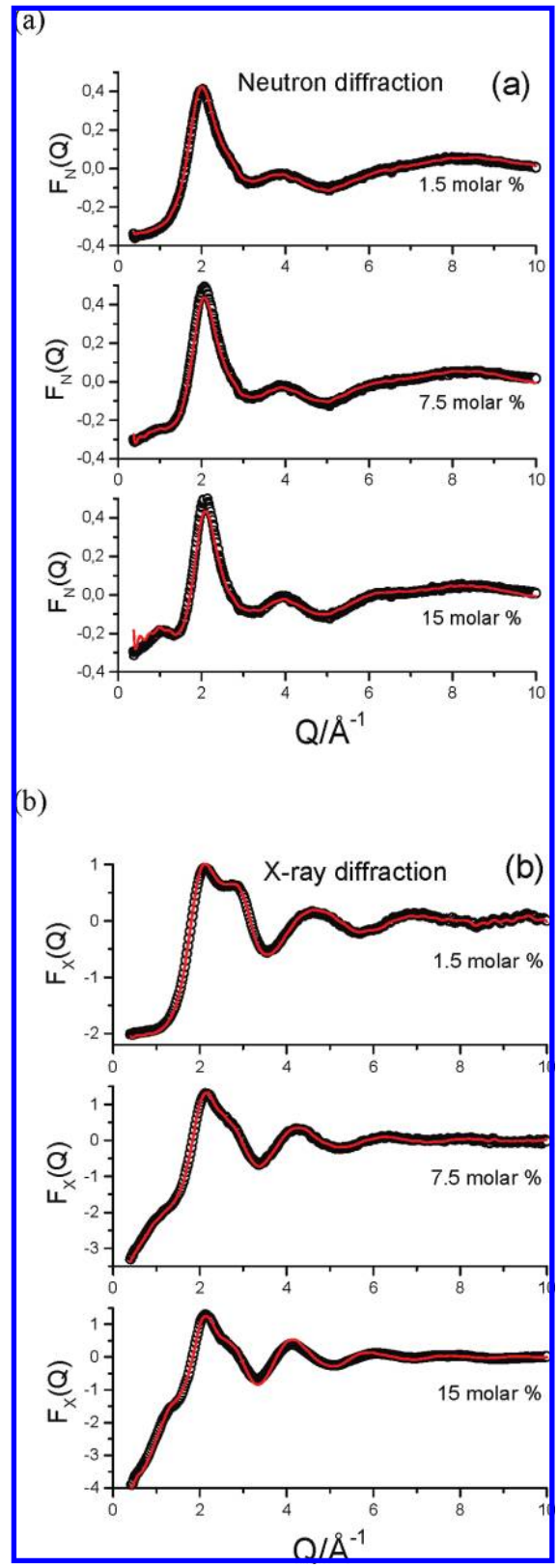

Figure 1. Total scattering structure factors from neutron (a) and X-ray (b) diffraction experiments (symbols), together with RMC simulated tssf's with (solid red line) and without (solid black line) applying prdf's from MD as input information.

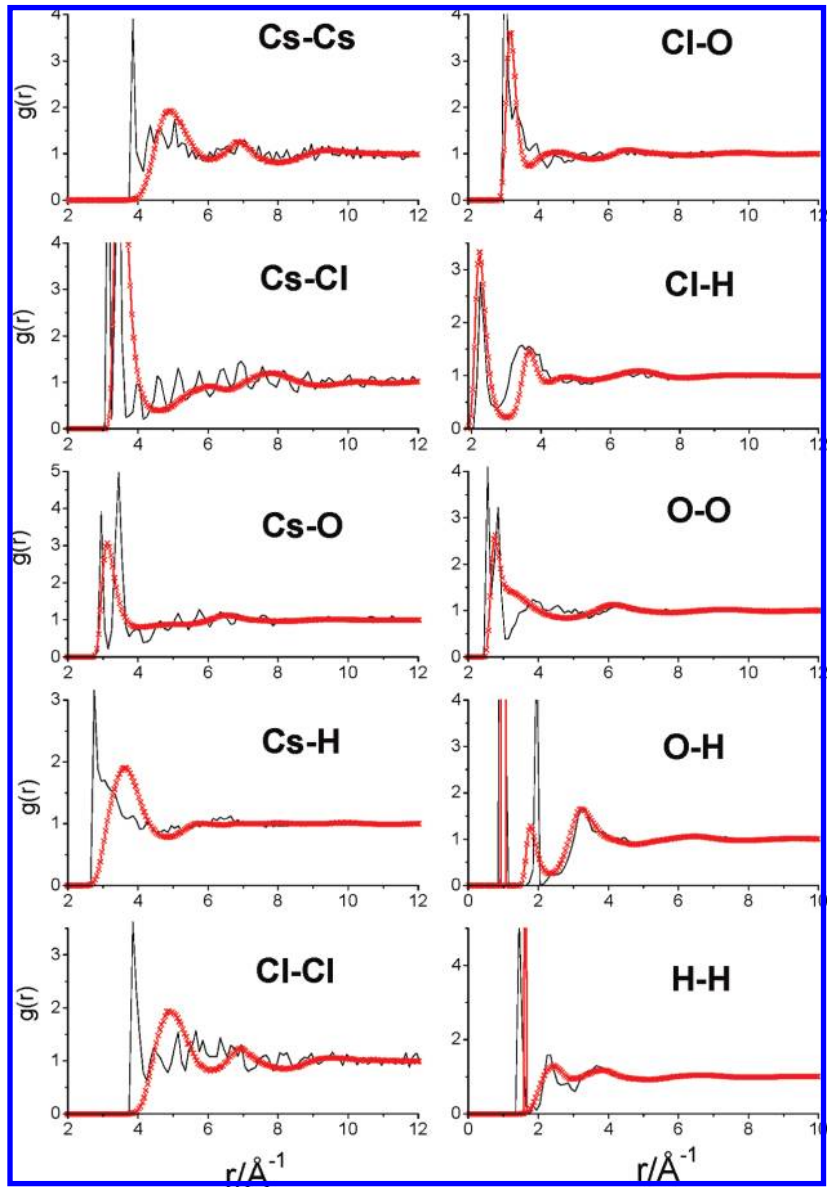

Figure 2. Partial radial distribution functions characterizing the FQ (black solid line) model and the molecular dynamics simulation using the SPC/E water potential (red solid line) at the highest salt concentration (15 mol %). Note that the $g_{ij}(r)$'s of the GR model are practically identical to those of the MD simulation.

considers that CsCl solutions in this study represent a case when 2 functions (the two experimental tssf's) are composed via mixing 10 "basis" functions (the prdf's). There are obviously very many possible mixtures of 10 prdf's that result in the same 2 tssf's—and the prdf's shown in Figure 2 for the FQ model represent one of these mixtures. One has to keep in mind, however, that these prdf', as well as the underlying structure, are fully consistent with measured diffraction data, a fact which in itself shows that the involvement of additional information into the interpretation of diffraction data for CsCl solutions is a must.

Another observation here to discuss is that the $g_{ij}(r)$'s from MD seem to differ completely from those obtained by the RMC-generated FQ model. The main question is the following: are the pair potential parameters chosen really useless for describing the structure of CsCl solutions? Figure 3 provides an approximate answer to this question: it shows a comparison between experimental data and neutron and X-ray weighted total $F(Q)$'s calculated from atomic coordinates of the GR model (in terms of prdf's, this model is identical to results of MD simulations). The—rather comforting—answer to the above question is self-evident: even though the agreement between experiment and MD simulation is far from perfect, with complete features missing from the simulated curves, the overall agreement may justifiably termed as "semiquantitative". That is, the particle arrangement generated by molecular dynamics simulation using a particular set of potential parameters[11,12] is nearly consistent with diffraction data.

Next we wish to investigate if the level of consistency with experiments can be enhanced. Figure 4 shows the example of, again, the highest concentration CsCl solution when using the FQ_OK calculation scheme. Obviously, the experimental data, as well as most of the prdf's are now approached to within errors; that is, our primary goal, producing structural models that—while reproducing experimental data—represent physically sensible and understandable partial pair correlations, could be achieved. This is a major benefit from applying the RMC-based scheme:[3] such structures could not have been prepared without that procedure. The FQ_OK models will later be used for more

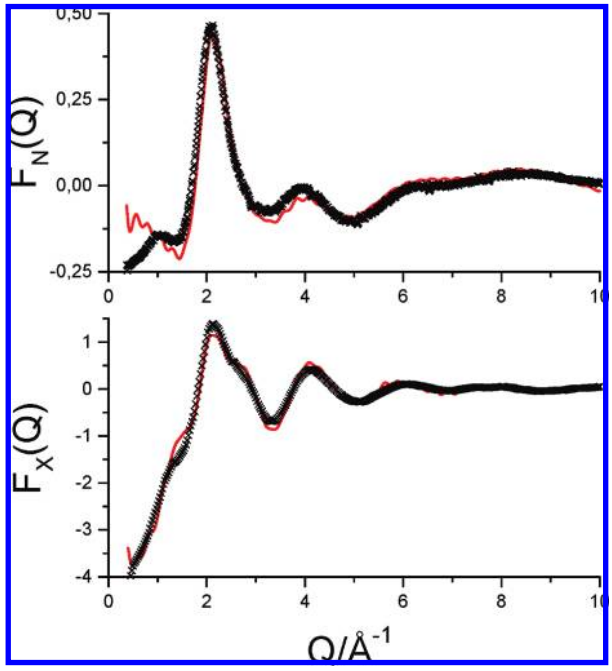

Figure 3. Comparison of experimental (symbols) neutron and X-ray weighted total scattering structure factors with those calculated from the GR model (red solid line) at the highest salt concentration (15 mol %).

detailed analyses of the structure; first, however, we will provide an in-depth discussion of Figure 4 and its implications.

Looking back to Figures 2 and 3, one might ask the following: how is it possible that out of a nearly hopeless situation, now we are at a rather promising one? It has to be noted first that such a remarkable level of consistency between experimental and MD simulated structural parameters could be achieved via the scheme applied here. The achievement, most likely, has been made at all possible by the fact that both tssf's and prdf's, being unique at the level of two-particle correlations only, allow a range of corresponding structures and the RMC procedure is an appropriate way of exploring if there are "overlaps" between these ranges of structures. Clearly, in each of the cases considered here (see below), such overlaps (at least at a semiquantitative level) have been found, as is proven by Figure 4. Note, however, that strictly speaking, the level of agreement with experimental data is always lower than when the experimental tssf's are modeled on their own. Still, it is fair to say that the general level of consistency with experiment appears to be beyond expectations.

By scrutinizing prdf's of Figure 4, the first impression may be that ion−water and even ion−ion correlations derived from MD simulations may be made fully consistent with experimental data. Concerning the widely spread belief, namely, that it is the ion−water potentials that pose the toughest challenge in the area of computer simulations of electrolyte solutions, this is perhaps the most unexpected finding. This statement is particularly valid if one considers a similar (although of much lower profile) study on rubidium bromide solutions[3,4] where ion−water prdf's proved to be fully *in*consistent with results of neutron diffraction experiments at high (but lower than in the case of CsCl solutions) concentration. This controversy urges us to carry out similar investigations in a systematic way, following with other Cs−halide solutions; indeed, a detailed study of aqueous CsBr solutions is already underway.

The next surprising observation is that it is the water-related prdf's, especially O−H and H−H, which are the least consistent

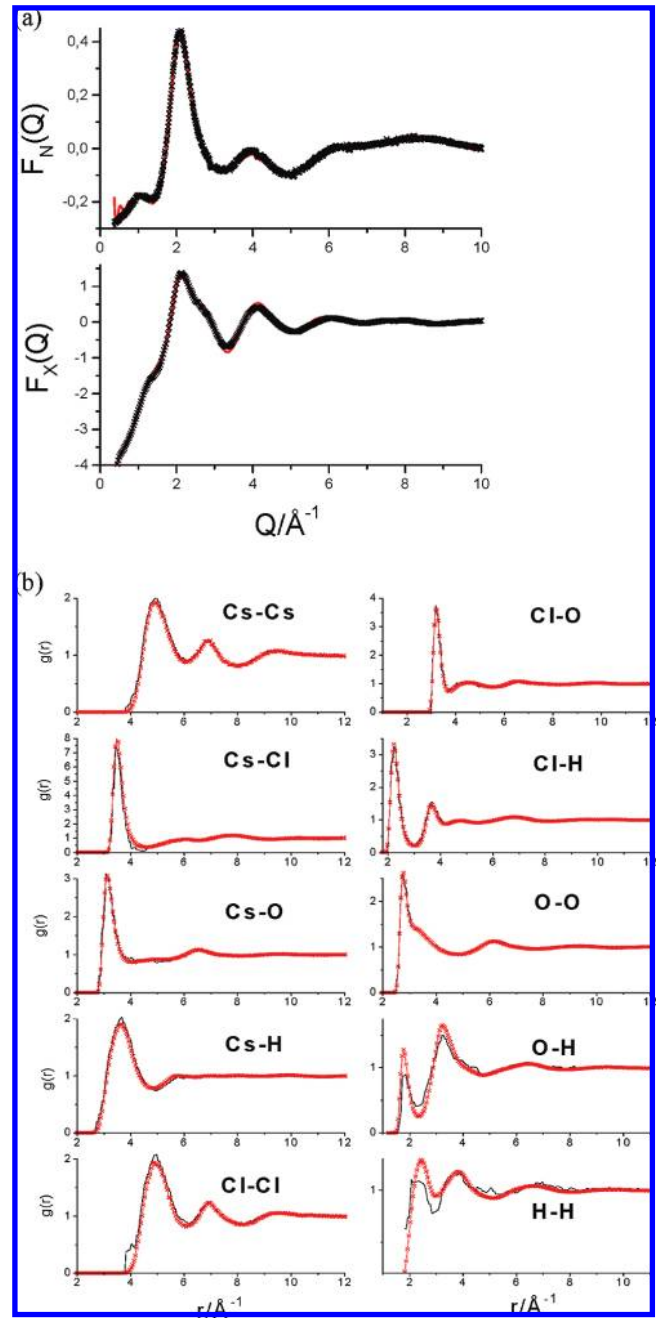

Figure 4. (a) Comparison of experimental (symbols) neutron and X-ray weighted total scattering structure factors with those calculated from the FQ_OK model (red solid line) at the highest salt concentration (15 mol %). (b) Comparison of MD simulated (red symbols) partial radial distribution functions with those calculated from the FQ_OK RMC model (black solid line) at the highest salt concentration (15 mol %).

with the two experimental tssf's. Note that only the intermolecular parts are fitted. As it is demonstrated by Figure 5, the same finding is valid at each salt concentration. On the face of it, this seems to be a smaller problem since there are many potential models to choose from; in addition, a fairly detailed investigation of water potentials has been carried out recently that applied the same (MD + RMC) scheme as is exploited here.[5] In that study, it was found that the TIP4P-2005 water potential[15] was slightly more consistent with neutron diffraction data of pure heavy water than the other potential parameters (including SPC/E). We therefore decided to repeat the molecular dynamics calculations mentioned in section 2.1, but this time using the TIP4P-2005 potential.

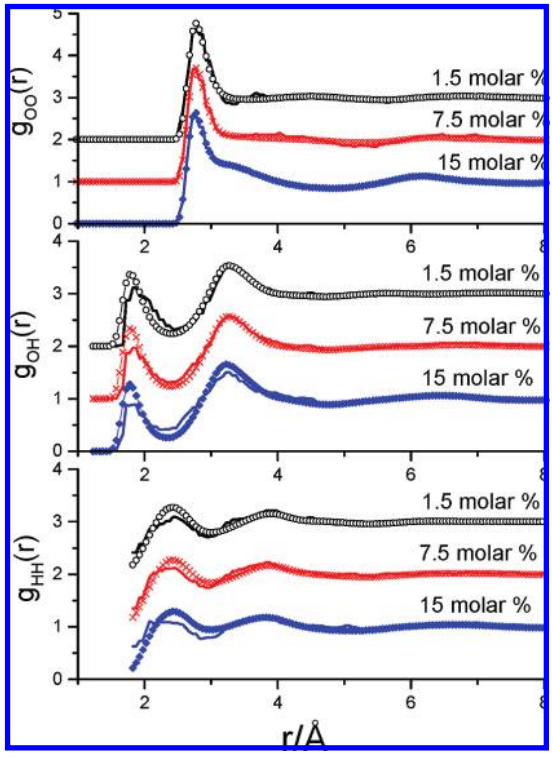

Figure 5. Partial radial distribution functions from FQ_OK RMC models (solid lines) characterizing water−water correlations at each concentration. (top panel) O−O. (middle panel) O−H. (bottom panel) H−H. (prdf's from MD simulations are also shown (symbols); water model: SPC/E.)

In terms of goodness-of-fit parameters, as well as of general appearance, this change of the water potential gave no improvement: it was still the water−water prdf's that were the most problematic. For the sake of a clearer presentation, we do not show figures of results for the TIP4P-2005 potential, very similar to Figures 1−5; instead, we present some unexpected subtle differences between the structures corresponding to the two (SPC/E and TIP4P-2005) water potential sets.

In Figure 6, Cl−O and Cl−H prdf's are displayed (for the higher concentration values; note that the curves are strongly magnified in comparison with those shown in Figure 5), for models GR, GR_OK, and FQ_OK, applying both water potentials. As it is obvious, all calculations led to nearly identical $g_{ij}(r)$'s up to the first minimum; this is true for most prdf's (at each salt concentration). However, around the first minimum a clear splitting of the curves is evident, leading to a phase shift around the second maximum: the SPC/E *water−water* potential requires (somewhat) shorter *second-neighbor anion−water* distances. Such a succinct difference would be impossible to detect without carrying out a structural analysis of at least the present detail. It should be recognized that both sets of prdf's are equally consistent with the two measured total scattering functions; that is, both (only slightly different) structures are equally possible, the available—limited—diffraction data cannot differentiate between them, due to the much larger number of prdf's (there are 10 of them) than tssf's (there are only 2 of them). Note that, on the other hand, RMC can explore the *range* of possible structures, which makes the method rather useful in similar situations (likely to be encountered most frequently in the area of complex liquids; see also section 1).

We now start the actual analyses of the structure of aqueous cesium chloride solutions, represented by the FQ_OK RMC structural models. It is important to stress here that the picture

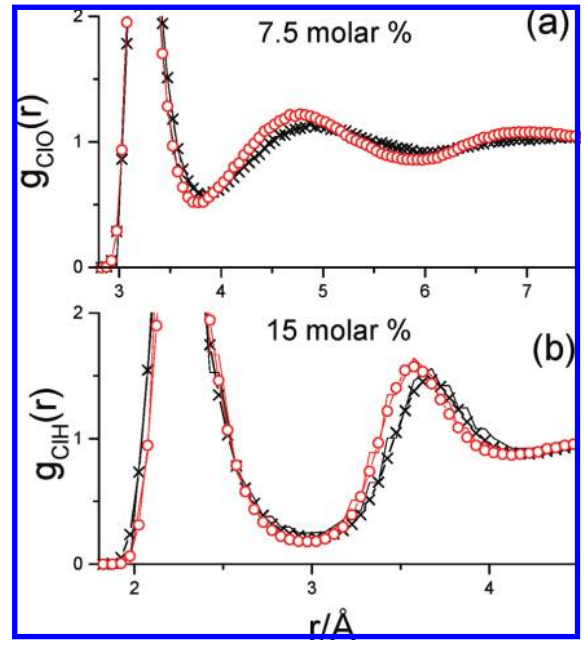

Figure 6. Comparison of Cl−O (top panel) and Cl−H (bottom panel) prdf's from GR (symbols) and FQ_OK (solid lines) RMC models using MD simulated results using both SPCE/E (black color code) and TIP4P-2005 (red color code) water potentials.

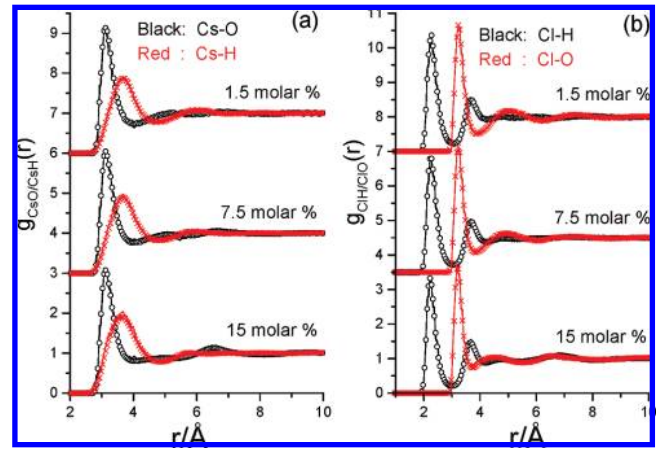

Figure 7. Partial radial distribution functions from FQ_OK models (solid lines) characterizing the solvation structure of ions at each concentration (prdf's from MD simulations are also shown (symbols); water model: SPC/E). (a) O and H atoms around the cation (Cs^+). (b) H and O atoms around the anion (Cl^-).

emerging from the analyses is *not* unique; it is just consistent with the two sets of diffraction data considered and the physics behind prdf's can be understood easily.

In Figure 7, partial radial distribution functions representing ion−water correlations are shown. Concerning the hydration of cations [Figure 7a], characteristics (peak position, peak height, peak width) of the first Cs−O and Cs−H peaks do not seem to change as concentration grows, indicating that concentration does not influence considerably the hydration sphere of cesium ions. If we look at average coordination numbers (Table 4), the average number of oxygen atoms in the first hydration sphere decreases from about 8.2 (1.5 mol %) to about 6.5 (15 mol %). These values are somewhat smaller than the 9.6 found for an infinitely dilute solution[12] and are in good agreement with the value of 7.9 found for a concentrated cesium iodide solution[24] by evaluating results of anomalous X-ray diffraction experiments. It may be noted, however, that the position of the Cs−O

TABLE 4: Average Partial Coordination Numbers as Calculated from FQ_OK RMC Models[a]

c (mol %)	1.5	1.5	7.5	7.5	15	15
water model	SPC/E	TIP4P-2005	SPC/E	TIP4P-2005	SPC/E	TIP4P-2005
Cs−O/4.0	8.18	8.22	7.40	7.59	6.53	6.47
Cs−H/4.8	27.04	27.10	25.05	25.22	23.00	22.92
Cl−O/3.8	6.98	6.68	5.96	5.91	4.88	4.75
Cl−H/3.0	6.42	6.00	5.47	5.22	4.51	4.33
O−O/3.2	3.87	3.86	3.35	3.28	3.02	2.99
O−H/2.4	3.76	3.75	3.24	3.21	3.17	3.19
H−H/3.0	5.85	5.82	5.34	5.24	5.20	5.34
Cs−Cs/6.0	0.72	0.81	1.95	1.91	3.45	3.52
Cs−Cl/4.2	0	0	0.97	0.84	2.24	2.11
Cl−Cl/6.2	0.48	0.64	2.13	2.02	3.44	3.19

[a] The upper boundary of the first coordination shell was set at the first minimum of the corresponding prdf and given after the "slash" (Å).

maximum was fixed at 3.0 Å in the latter work, whereas it was 3.1 Å here without any external intervention. It is also worth mentioning that although it is hard to find any well-defined feature in the prdf's from the FQ RMC model, Cs−O and Cs−H coordination numbers (just as other coordination numbers) are in a very good agreement with those calculated from the FQ_OK RMC models. Interestingly, the number of H atoms found up to the first minimum of the Cs−H prdf is always much higher than the double of the number of O atoms, which indicates that the boundaries of the Cs−O and Cs−H shells are not too well-defined. Indeed, the $g_{CsO}(r)$ value at the first minimum is about 0.8 for the least concentrated solution and gets very close to unity as concentration grows; in this respect, the Cs−H shell is more distinct. The distribution of the cosines of Cs···O−H angles (where "···" and "−" refer to nonbonded and bonded particle pairs, respectively), which characterizes the orientation of water molecules with respect to the cation, has only a very broad hump (not shown) at cosines corresponding to angles between 80 and 110°. This feature is even less well-defined than that found for the rubidium cation in rubidium chloride solutions.[25] This finding also supports the picture of a nonuniform, not regular cation hydration sphere.

The hydration shell of the chloride ion is dominated by the very well-defined Cl−H first neighbor distance at about 2.2 Å and the first minimum at about 3 Å, where the corresponding value of the Cl−H prdf is close to zero. These characteristics do not change upon increasing concentration, although the number of H atoms in this neat shell decreases from about 6 to about 4.5 (see Table 4), which is due to the strongly decreasing number of water molecules/ion. The Cl−O first coordination sphere is more disordered, as the quite high (and growing, as concentration increases) value of $g_{ClO}(r)$ at the first minimum signifies. Also, the number of O atoms in the first Cl−O sphere is somewhat higher than the number of H atoms in the first Cl−H sphere, decreasing from about 7 at the lowest concentration to a little less than 5. That is, contrary to what was suggested in ref 25, every O atom in the first shell has one H atom pointing toward the anion. The orientation of coordinated water molecules can be characterized by the distribution of the cosines of Cl···H−O angles (see Figure 8a). These distributions are dominated by the presence of straight (180°) angles at each concentration; the occurrence of such regular angles is more probable the more dilute the solution is. This finding indicates that increasing the concentration of the salt distorts the anion hydration shell, which is perhaps a somewhat unexpected outcome.

It is instructive to review different views of chloride ion hydration (see, e.g., refs 8 and 25−31). The Cl−O coordination

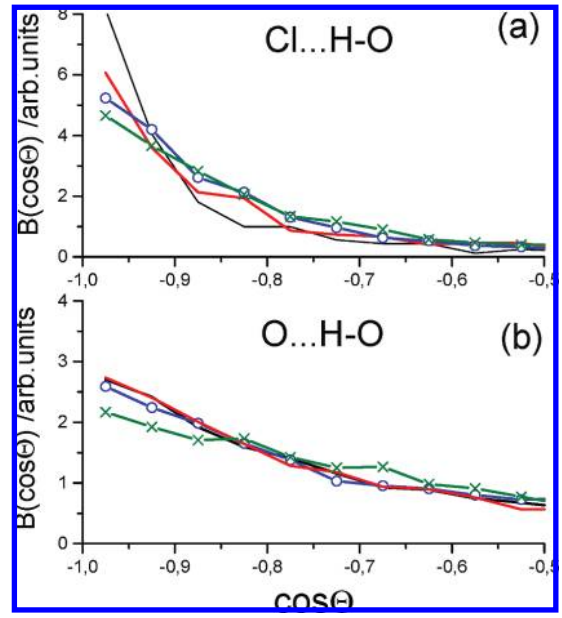

Figure 8. Distribution of cosines of Cl···H−O (a) and O···H−O (b) angles. (black solid line) 1.5 mol % with SPC/E; (red solid line) 1.5 mol % with TIP4P-2005; (blue line with symbols) 15 mol % with SPC/E; (olive line with symbols) 15 mol % with TIP4P-2005.

numbers are of roughly the same order as found here; the Cl−H coordination numbers, however, range between 3[25] and 6.5.[29] The present results are closer to the more regular suggestions, implying a value of around 6 (see Table 4). Note, however, that already the FQ RMC model, applying no extra information for Cl−H correlations, provided this value for CsCl solutions. For RbCl solutions, on the other hand, it was impossible to achieve such a high Cl−H coordination number in an RMC calculation using very strong coordination constraints for the Cl−H pair. That is, it is possible that the coordination of the chloride ion depends on the counterion, a conjecture which is expected to be particularly relevant at higher concentrations.

Partial radial distribution functions related to the water "subsystem" (water−water correlations) were shown in Figure 5. As it has already been discussed above, these are the prdf's that are the least similar to those obtained from MD simulations. At the lowest concentration, for instance, not even the position of the first intermolecular O−H peak could be reproduced if consistency with experimental data was to be maintained; this indictates that this part of the pair potential needs to be improved. Nevertheless, all the water−water coordination numbers (O−O, O−H, and H−H; see Table 4) are in good agreement with the original MD results. The average number of water molecules around a water molecule decreases from about 3.8 to about 3 as the salt concentration increases from 1.5 to 15 mol %, as it can be devised from the O−O coordination number. The average number of H atoms around an O atom follows this change very closely, which means that all the water molecules are hydrogen bonded, since there is always an H atom between two neighboring O atoms. The distribution of the cosines of H···O−H angles (Figure 8b) shows that higher CsCl concentration results in a lower ratio of regular hydrogen bond angles. That is, in accordance with commonsense expectations, as well as with earlier studies,[25,32] the hydrogen bond network of water molecules becomes more distorted with increasing salt concentration.

There is one more aspect of the microscopic structure which needs to be discussed when dealing with highly concentrated

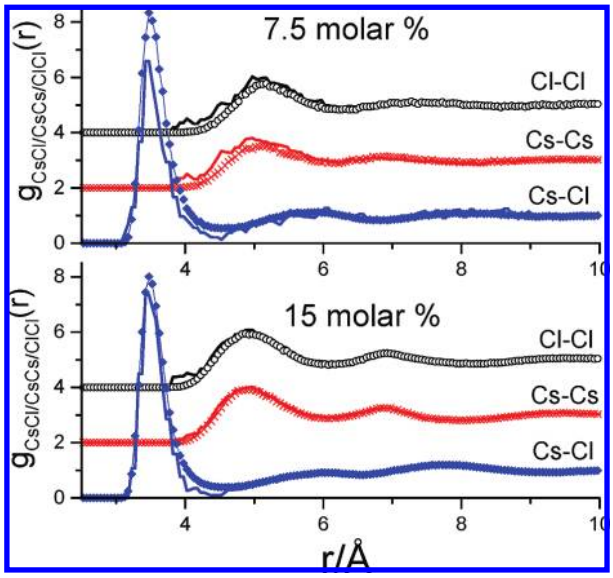

Figure 9. Partial radial distribution functions from FQ_OK models characterizing ion−ion correlations at the higher concentration values [7.5 (top panel) and 15 mol % (bottom panel)] (prdf's from MD simulations are also shown; water model: SPC/E).

salt solutions: this is the—rather difficult and controversial—issue of ion−ion correlations ("ion-pairing"). Figure 9 displays ion−ion partial radial distribution functions at concentrations of 7.5 and 15 mol % (at the lowest concentration value, there were too few ions for obtaining reliable data). Like−like ionic prdf's are quite similar to each other and also, the Cs−Cl prdf seems to be not very much affected by concentration above 7.5 mol %. It is obvious that, peaking at about 3.5 Å, counterions do appear in each other's first coordination shell; this is agreement with the finding of ref 24. The number of counterions in the first coordination sphere of ions is about one at 7.5 mol % and grows to about two at 15 mol % (there are no counterions at these short distances in the most dilute solution). This growth almost exactly equals the loss of water molecules from the first coordination shell during the concentration increase; that is, counterions do seem to replace water molecules. This replacement brings about changes in terms of the local charge distribution which, in turn, causes the distortion of the structure of hydration spheres detected in the present study.

4. Conclusions

We have investigated the structure of cesium chloride solutions in (heavy) water, over a wide range of the salt concentration, using the combination of neutron and X-ray diffraction experimental data with molecular dynamics simulations via a reverse Monte Carlo based scheme introduced recently.[3] Such an approach is useful for studies of complex systems, which almost always contain more than three atomic species. For such multicomponent systems, obtaining complete structural information from diffraction measurements is impossible at present. The knowledge about the microscopic structure of electrolyte solutions may be enhanced by performing additional experiments using the EXAFS technique. This possibility has not been explored in the present work; in a future investigation, we will explore this possibility. For the electrolyte solutions in question, computer simulations with model interaction potentials will gain more emphasis and the need for validating results from them will become even more important.

Concerning aqueous CsCl solutions, we could unambiguously show that the simple ion−water and ion−ion pair potentials applied during the MD simulations provide partial radial distribution functions that are consistent with experimental data over the entire concentration range. It seems, however, that pair interactions between water molecules need to be described more accurately. Changing the water interaction potential from the widely used SPC/E model to the more recent TIP4P-2005 one did not improve the situation. Therefore, one needs to attempt performing simulations using flexible models and combine them with present experimental data and RMC modeling. However, strong arguments are necessary for the design of ion−water interaction potentials, independent of the choice of water potentials. Possibly, spectroscopic measurements can contribute to the better understanding of this issue.

By analyzing particle configurations from the most successful FQ_OK reverse Monte Carlo models, we found the following features of the structure of cesium chloride solutions:

(a) The average number of water molecules around a given water molecule decreases from a little less than four to about three as concentration increases to its near-saturation value. Each surrounding water molecule is hydrogen bonded to the central one, although the distortion of the hydrogen bonded network of the solvent subsystem is evident.

(b) The average number of water molecules around cations decreases from about 8 to about 6.5 as concentration increases from 1.5 to 15 mol %, whereas the same quantity for the anions changes from about 7 to about 5.

(c) While the hydration shell of cesium ions is rather diffuse, water molecules around chloride ions seem to be neatly oriented.

(d) The average angle of Cl···H−O particle arrangements, characteristic to anion−water hydrogen bonds, is closer to 180° than that found for O···H−O arrangements (water−water hydrogen bonds).

(e) As concentration increases, counterions appear in the first coordination sphere of the ions. At the highest concentration, close to saturation, the number of counterions in the vicinity of ions is about two.

On the basis of the above, it was possible to reveal a simple mechanism, consistent with diffraction data, for the distortion of the structure of the hydration shells of ions: as salt concentration increases, one (or at very high concentrations, two) water molecule(s) in the hydration shell is (are) replaced by counterion(s), leading to the formation of "ion pairs". This process has influence on the behavior of the surrounding water molecules.

We note that most probably, similar conclusions may have been drawn already from the analyses of prdf's obtained from MD simulations; however, without the RMC-based scheme,[3] the validation of these conclusions would not have been possible.

There are a number of open questions that require further investigations. Some of them we have mentioned above. In particular, it would be desirable to investigate the dependence of the structure of ionic hydration shells on the chemical identity of the counterion. For clarifying this issue, studies on cesium bromide and cesium iodide solutions are underway. It might also be beneficial if the resulting structures could be further relaxed by some ab initio algorithm, so that not only the structure but also the "energetics" would be as realistic as possible; for the foreseeable future, however, such an approach will remain prohibitively expensive computationally.

Acknowledgment. We thank Drs. Shinji Kohara (SPring-8, Japan; BL04B2 in the 2004A period) and Anders Wannberg (Studsvik NFL, Sweden) for their invaluable help with the X-ray and neutron diffraction experiments. L.P., H.D., and O.P. are

grateful for a bilateral travel grant of the CONACyT of Mexico and the Hungarian Academy of Sciences. O.P. and H.D. have been partially supported by DGAPA of the UNAM, Nos. IN223808-2 and IN102207. V.M. and L.P. have also been also supported by the Hungarian Basic Research Fund (OTKA), Grant No. T048580.

References and Notes

(1) See, e.g., (a) Friedman, H. *Ionic Solution Theory, Based on Cluster Expansion Methods*; Interscience Publishers: New York, 1962. (b) Falkenhagen, H., Ebeling, W., Hertz, H. G. *Theorie der Elektrolyte*; S. Hirzel (Verlag): Leipzig, 1971. (c) *Water, a Comprehensive Treatise*; Franks, F., Ed.; Plenum Press: New York, 1973; Vol. 3. (d) Heinzinger, K. In *Computer Modelling of Fluids, Polymers and Solids*; Catlow, C. R. A., Parker, S. C., Allen, M. P., Eds.; Kluwer Academic Publishers; Doordrecht, 1990; p 357. (e) *The Physics and Chemistry of Aqueous Ionic Solutions*; Bellisent-Funel, M.-C., Neilson, G. W., Eds.; NATO ASI Series C; Reidel: Dordrect, Netherlands, 1987; Vol. 205. (f) Barthel, J., Krienke, H., Kunz, W. *Physical Chemistry of Electrolyte Solutions: Modern Aspects*; Springer Verlag: Darmstadt, 1998.

(2) Allen, M. P.; Tildesley, D. J. *Computer Simulation of Liquids*; Clarendon Press: Oxford, 1987.

(3) Pusztai, L.; Harsányi, I.; Dominguez, H.; Pizio, O. *Chem. Phys. Lett.* **2008**, *457*, 96.

(4) Pusztai, L.; Dominguez, H.; Pizio, O.; Sokolowski, S. *J. Mol. Liq.* **2009**, *147*, 52.

(5) Pusztai, L.; Pizio, O.; Sokolowski, S. *J. Chem. Phys.* **2008**, *129*, 184103.

(6) Soper, A. K. *J. Phys.: Condens. Matter* **2007**, *19*, 335206.

(7) Soper, A. K. *Phys. Rev. B* **2005**, *72*, 104204.

(8) Soper, A. K.; Weckström, K. *Biophys. Chem.* **2006**, *124*, 180.

(9) McGreevy, R. L.; Pusztai, L. *Molec. Simul.* **1988**, *1*, 359.

(10) Forester, T. R.; Smith, W. *DL-POLY Package of Molecular Dynamics Simulation*; CCLRC, Daresbury Laboratory: Warrington, 1996.

(11) Berendsen, H. J. C.; Grigera, J. R.; Straatsma, T. P. *J. Phys. Chem.* **1987**, *91*, 6269.

(12) Lee, S. H.; Rasaiah, J. C. *J. Phys. Chem.* **1996**, *100*, 1420.

(13) Dang, L. X. *Chem. Phys. Lett.* **1994**, *227*, 211.

(14) Smith, D. E.; Dang, L. X. *J. Chem. Phys.* **1994**, *100*, 3757.

(15) Abascal, J. L. F.; Vega, C. *J. Chem. Phys.* **2005**, *123*, 234505.

(16) McGreevy, R. L. *J. Phys.: Condens. Matter* **2001**, *13*, R843.

(17) Evrard, G.; Pusztai, L. *J. Phys.: Cond. Matter* **2005**, *17*, S1.

(18) Gereben, O.; Jóvári, P.; Temleitner, L.; Pusztai, L. *J. Optoelectr. Adv. Mater.* **2007**, *9*, 3021.

(19) Keen, D. A. *J. Appl. Crystallogr.* **2001**, *34*, 172.

(20) Pusztai, L.; Harsányi, I.; Wannberg, A.; Kohara, S.; Sheptyakov, D., 2009, private communication.

(21) Wannberg, A.; Mellergård, A.; Zetterström, P.; Grönros, M.; Karlsson, L.-E.; McGreevy, R. L. *J. Neutron Res.* **1999**, *8*, 133.

(22) (a) Isshiki, M.; Ohishi, Y.; Goto, S.; Takeshita, K.; Ishikawa, T. *Nucl. Instrum. Methods Phys. Res. A* **2001**, *467−468*, 663. (b) Kohara, S.; Itou, M.; Suzuya, K.; Inamura, Y.; Sakurai, Y.; Ohishi, Y.; Takata, M. *J. Phys.: Condens. Matter* **2007**, *19*, 506101.

(23) Kohara, S.; Suzuya, K; Kashihara, Y.; Matsumoto, N.; Umesaki, N; Sakai, I. *Nucl. Instr. Meth. A* **2001**, *46*, 7468, 1030.

(24) Ramos, S.; Barnes, A. C.; Neilson, G. W.; Buchanan, P. *J. Chem. Phys.* **2005**, *122*, 214501.

(25) Harsányi, I.; Pusztai, L. *J. Phys.: Condens. Matter* **2007**, *19*, 335208.

(26) Narten, A. H.; Vaslow, F.; Levy, H. A. *J. Chem. Phys.* **1973**, *58*, 5017.

(27) Cummings, S.; Enderby, J. E.; Neilson, G. W.; Newsome, J. R.; Howe, R. A.; Howells, W. S.; Soper, A. K. *Nature* **1980**, *287*, 714.

(28) Bopp, P. A.; Okada, I.; Ohtaki, H.; Heinzinger, K. *Z. Naturforsch.* **1985**, *40a*, 116.

(29) Driesner, T.; Cummings, P. T. *J. Chem. Phys.* **1999**, *111*, 5146.

(30) Jal, J. F.; Soper, A. K.; Carmona, P.; Dupuy, J. *J. Phys.: Cond. Matter* **1991**, *3*, 551.

(31) Copestake, A. P.; Neilson, G. W.; Enderby, J. E. *J. Phys. C: Solid State Phys.* **1985**, *18*, 4211.

(32) Harsányi, I.; Pusztai, L. *J. Chem. Phys.* **2005**, *122*, 124512.

JP900092G